

Effects of Temporary Color Steel Buildings on Urban Development and Urban Space Form in China

Shuwen Yang^{1,2,*}, Haowen Yan^{1,2}, Yikun Li^{1,2} and Yi He²

1 Faculty of Geomatics, Lanzhou Jiaotong University, Lanzhou 730070, China; ysw040966@163.com (S.Y.); yhw0118@qq.com (H.Y.); liyikun2003@hotmail.com(Y.L.)

2 National-Local Joint Engineering Research Center of Technologies and Applications for National Geographic State Monitoring, Lanzhou 730070, China; 764324437@qq.com (Y.H.)

* Correspondence: ysw040966@163.com; 825198827@qq.com

Abstract: The detection of temporary color steel buildings and the analysis of their spatiotemporal patterns and characteristics are of great importance in many developing cities, because areas densely distributed with color steel buildings are usually problematic regions with high population density, sustainable development and risk level, which are challenging for local governments. Using the high-resolution satellite images of the Anning District, Lanzhou City, China as the case study, this paper first extracts the information of the color steel buildings for two different periods. Then the spatiotemporal distributional characteristics of the color steel buildings are analyzed, both at small scale (temporary buildings) and large scale (planthouses, warehouses, etc.). Finally, this paper utilizes kernel density estimation, Delaunay triangulation and Voronoi diagrams to examine the spatial distribution, aggregation and proximity characteristics of the color steel buildings. Our experiments show that the temporal and spatial differences of urban development, the phased characteristics and urban space are represented by various types of color steel buildings. Thus, there are some robust coupling relationship between color steel buildings, urban spatial form and urban development.

Keywords: color steel buildings; urban space form; high-resolution satellite imagery; Lanzhou

*

1. Introduction

Buildings are strongly related to the urban space form [1-3] and urban functional zones [4]. The issues of urban planning, governmental policies, population changes, urban environmental issues, socio-economic development, and other cultural values are directly or indirectly reflected by the changes of urban space form and urban landscape [5-7]. Moreover, the internal imbalance of urban areas, the spatial distinctions of urban development, the extent of development as well as other issues are also reflected by buildings [8-9].

Color steel buildings (CSBs), including factories and kiosks, warehouses, temporal sheds, and temporary residential houses, are very common in the suburban areas of many developing cities of China [10]. In recent years, CSBs have also been temporarily constructed in new economic development zones, urban fringes and urban villages. The areas with large number of CSBs have received much concerns from governments and NGOs due to the high fire and crime risks, serious pollution and weak livable environment in these areas. Besides, the number of CSBs, spatial distribution and aggregation characteristics of CSBs have close relationship with the internal imbalance of urban function, the differences of population structure, and the level of urban economic development.

Since CSBs are relatively small in more developed cities and have attracted less attention from scholars' part. By now the changing relationships between urban space form and CSBs have not been found in recent literatures. However, some studies utilize roads, green areas and nighttime lighting to study urban problems [11-13]. For example, spatial structure and landscape of a city can be effectively represented by the density of residential areas and commercial development [14-15]. Based on DMSP/OLS, NPP-VIIRS and SPOT-VGT image data, the characteristics and dynamics of urban expansion are extracted and analyzed [16-17]. Other studies utilized high-speed railways to analyze the evolution and impact of urban aggregations and urban space form [18-20].

In some related studies, kernel density estimation has been widely used for spatial density evaluation which considers the decay impact of services based on Tobler's First Law of Geography. For example, some work uses kernel density estimation to analyze central business districts [21], spatial distribution characteristics of healthcare facilities [22-23], and crime prediction [24-26]. In some work the Delaunay and Voronoi methods have been adopted for exploring spatial distribution, influence scope, and proximity of geographic entities [6, 27-28]. Some studies have analyzed urban land spatial pattern based on an extended Voronoi diagram [29]. Other study investigated spatial aggregation and generalization of massive movement data [30].

Like road network [31-32], green space [33], commercial area, urban functional zones [34], scenic spots, etc., CSBs are a part of urban landscape, and their spatial distribution and aggregation characteristics can effectively express the characteristics of urban spatial structure. However, there is still a lack of such work. To resolve this issue, in this study, information on CSBs is extracted from GF-2 high-resolution images and Quickbird-2 images, and the spatial and temporal distribution and spatial aggregation characteristics of CSBs in the Anning District, Lanzhou City are analyzed with the kernel density estimation and Delaunay-Voronoi methods. Results of this study can help to reveal how CSBs affect urban spatial structure and sustainable urban development from a new perspective.

2. Study area and data

2.1 Study area

The study area is one part of the Anning District of Lanzhou City, which is the capital city of Gansu Province and located in a typical valley in western China. As shown in Figure 1, the area is located on the north of the Yellow River, and also is distributed in strips.

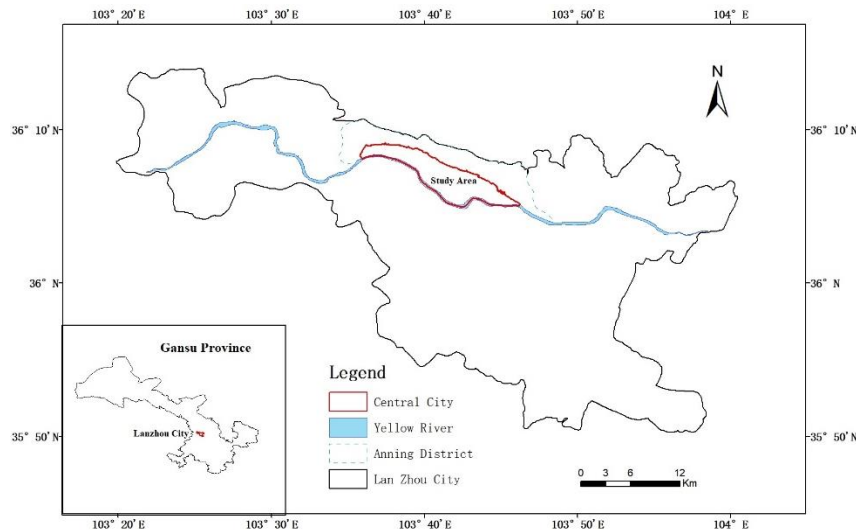


Fig. 1. Location of the study area

The district has been recently built, but its development speed is very rapid in recent years. The large enterprises in the district are clustered and form a unique economic and technological development zone, which is ranked national-level in China. The district is full of educational institutions (such as school, college and university), and many large-scale parks. Therefore, the greenery proportion is relatively high.

At present, urban transformation and upgrading is undergoing in the Anning district. Temporary CSBs are widely spread in the new technology development areas, urban fringes, urban-rural junctions and urban villages. The densely distributed CSBs are mainly temporary residential building tops and new technology development zones including small and medium-sized warehouses and carports (Figure 2). Therefore, this area is chosen as the study area.



Fig. 2. Photos of color steel buildings

2.2 Data

To analyze the characteristics of the spatial-temporal changes of CSBs in the study area, this study selects Chinese GF-2 satellite and US Quickbird-2(QB-2) images for CSBs extraction. The GF-2 imagery was 4m in multi-spectrum bands and 1m in panchromatic band, and acquired on 2017-08-04. The QB-2 imagery was 2.44m in multi-spectrum bands and 0.61m in panchromatic band and acquired on 2005-10-25. Of them, the multi-spectral images of GF-2 and QB-2 are the original images, which include four bands, blue-light band, green-light band, red-light band and near infrared band.

3. Methods

Through preliminary analysis of the CSBs and remote sensing interpretation, it is found that spatial aggregation characteristics of the CSBs are relatively obvious. For further analysis, we used geographical statistics analysis, kernel density estimation (KDE) and Delaunay-Voronoi method to analyze the aggregation characteristics, spatial distribution and proximity of the CSBs. Figure 3 shows the technical route of CSBs' extraction and analysis and includes three steps:

CSBs extraction from VHR images, and analyses of spatiotemporal change and aggregation characteristics.

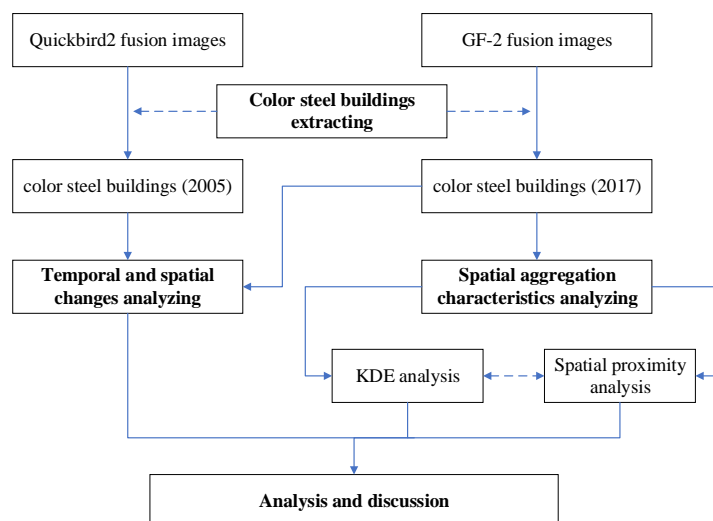


Fig. 3. The technology route of color steel buildings' extraction and analysis

3.1 CSB extraction

The CSBs are distributed dispersedly, and their sizes, heights and types differ greatly. Abundant spatial information is contained in high-resolution satellite remote sensing imagery. Therefore, these images can be effectively utilized to extract the CSBs.

Since the individual area of the CSBs is relatively small, therefore the GF-2 and QB-2 images were first matched and fused to improve the resolution and interpretation accuracy. The spatial resolution of the GF-2 fused images is 1 meter, and QB-2 fused images is 0.61 meter. Second, the manual interpretation method was utilized to extract CSBs. Finally, the corresponding area for further analysis and processing was utilized to classify and code the extracted information on CSBs.

In summary, the specific algorithm flow of CSBs' extraction is shown in Figure 4.

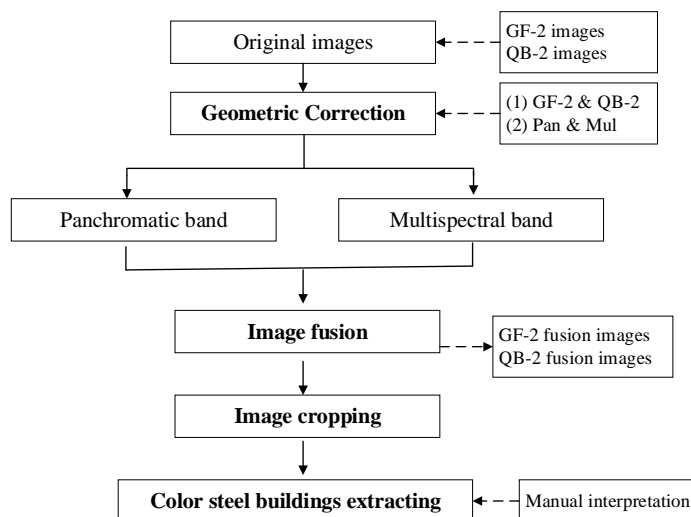


Fig. 4. The technology route of color steel buildings extraction

GF-2 images used in this study are shown in Fig. 5 and Fig.6. The different types of CSBs are represented by blue, white and green map spots. Figure 5(a) is an image of Lanzhou city university (LCU), the experimental secondary school (ESS), Liujiapu primary school and the surrounding area. The CSBs in this area are mainly located in urban villages which are distributed

around the universities and secondary schools according to the field surveys. Most of them are small CSBs which are utilized for temporal residence and commercial purposes. Figure 5 (b) shows the extracted outlines of the CSBs. An image of Gansu Snow Brewery near the site is shown in Figure 6(a). Large-scale CSBs such as warehouses, companies' plants and factories, occupy most of the area which is located within the New Technology Development Zone in Anning District of Lanzhou City. The extracted color steel building information is shown in Figure 6 (b).

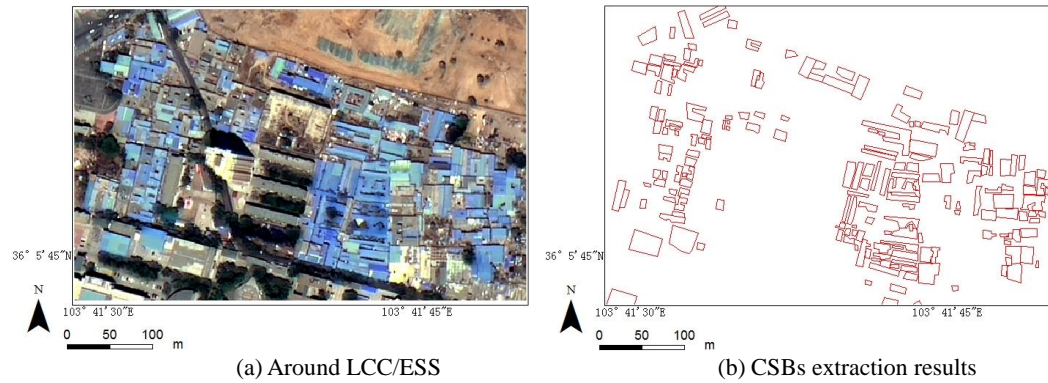


Fig. 5. Small CSBs extraction based on GF-2 images

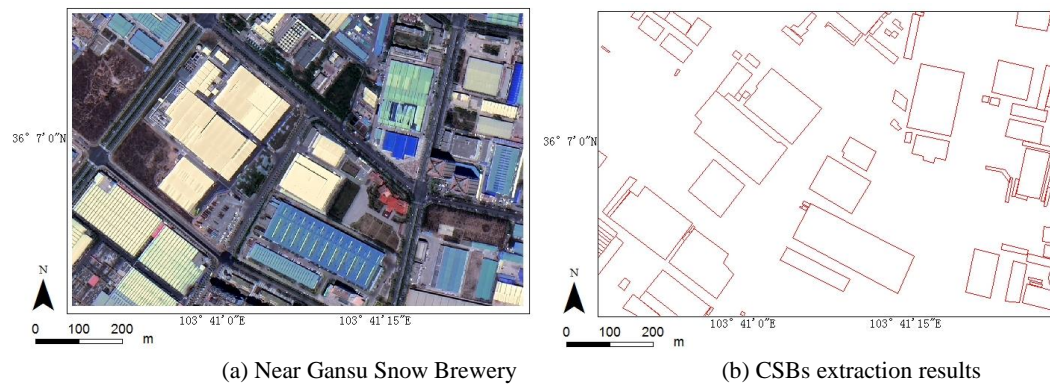


Fig. 6. Large CSBs extraction based on the GF-2 images

3.2 Kernel density estimation

In point pattern analysis [35-36], KDE is an effective method and the situation, in which the center radiation value is positively proportional to the closeness to the core, can be effectively described by the results of KDE calculation [37-38]. It calculates and exports point density of each grid cell by using a moving window. The KDE method was used in this study to analyze the aggregation and spatial distribution characteristics of CSBs.

To perform KDE, the optimal calculation approach is defined as:

$$f(s) = \sum_{i=1}^n \frac{1}{h^2} k\left(\frac{s-c_i}{h}\right) \quad (1)$$

where $f(s)$ is the kernel density calculation function at spatial position s . h is a bandwidth, which measures the distance attenuation threshold. The number of element points is n , whose distance from position s is equal to or less than h . The weight function is defined as k function, in which 4 space weight equations are most commonly used (Eq. 2).

$$k\left(\frac{s-c_i}{h}\right) = \frac{3}{4} \left(1 - \frac{(s-c_i)^2}{h^2}\right) \quad (2)$$

According to relevant studies [39-40], the density analysis results are only slightly affected by the weight function. Moreover, the analysis scale and specific issues that directly affect the results of the density analysis are used to determine the bandwidth (h) value.

3.3 Delaunay-Voronoi Diagram analysis

The first law of geography states [41] that the information in one spatial unit is related with the information in the surrounding units, and the units with small distance have large relatedness. A geographic aggregation is a collection of multiple single objects due to high local spatial association. A boundary of an aggregation may describe the shape and spatial distribution of the group.

Related studies show that the uniqueness and empty circle characteristics of the Delaunay triangulation can correctly represent the spatial proximity between geographical entities. The Voronoi diagram, also known as the Tyson polygon, is a dual graph of the Delaunay triangulation [42]. It consists of a set of consecutive polygons, which consist of perpendicular bisectors connecting two adjacent points. The plane is divided according to the nearest neighbor principle. The distance from the point in each polygon of the Voronoi diagram to the corresponding scatter point is closer than the distance from other scatter points [43]. Therefore, the Delaunay-Voronoi analysis method can effectively study the spatial distribution, influence scope, and proximity of geographic entities [27]. According to the study, the area size of the Voronoi diagram and the triangular side length of the Delaunay triangulation represent the spatial distribution characteristics and density, distance, and other neighboring features of the color steel buildings.

The Delaunay triangulation has several generation methods, such as point-by-point interpolation, triangulation, and score algorithms. Due to the strong aggregation characteristics of small CSBs, we adopted the constraint Delaunay triangulation algorithm [44]. According to the field investigation and analysis, the threshold of the geometrical center distance of the color plate (Delaunay triangulation side length) is constrained. Therefore, this approach minimizes the size of the TIN (Triangulated Irregular Network) to guarantee that every vertex and edge of the Delaunay triangulation contains the properties and spatial relationships of the color buildings.

4. Results and analyses

4.1 Analysis of temporal and spatial changes

Based on Quickbird2 images of 2005-10-25 and GF-2 images of 2017-08-04, a manual interpretation method was used to extract CSBs in Anning District, Lanzhou City. The experimental results are depicted in Figure 7.

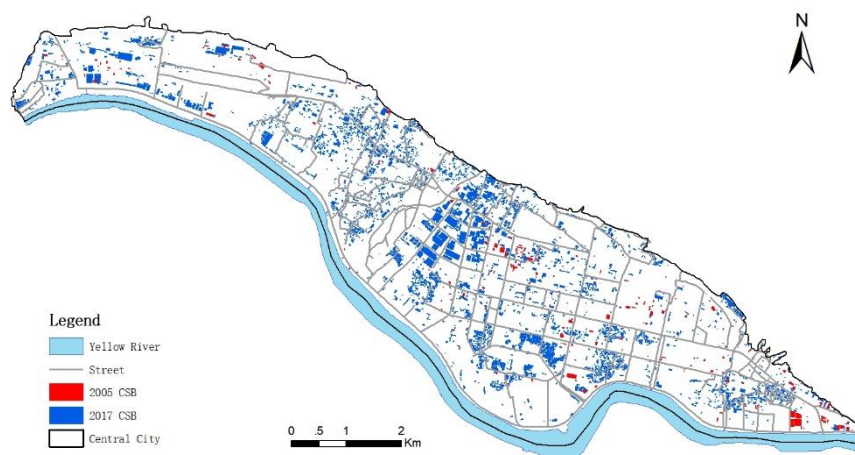


Fig. 7. Results of CSBs extraction in the main urban area of Anning District, Lanzhou City

As shown in Figure 7, there were only few CSBs in 2005 (red map spots, QB-2 imagery) compared with that in 2017 (blue map spots, GF-2 imagery).

Taking Wangjiazhuang Village as an example (Figure 8), only 2 CSBs were distributed in this area in 2005, but more than 130 CSBs were built in 2017. It is clear that there was an extremely significant increase of CSBs from 2005 to 2015. Areas with increased number of CSBs are

generally located in the urban villages and new technology development zones.

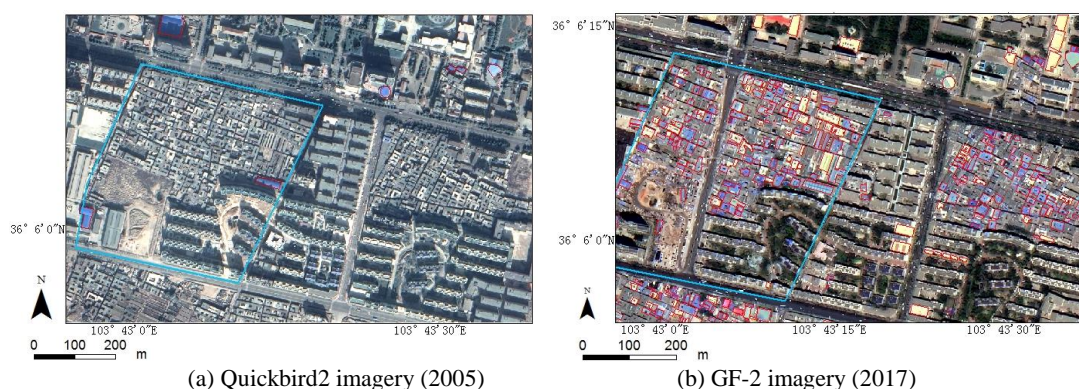


Fig. 8. Increase of CSBs number from 2005 to 2017

According to further statistics (Fig. 9), only 265 CSBs were extracted in the study area in 2005, and 6,559 CSBs were obtained in 2017. Based on the field research, image interpretation and analysis in 2017, the following conclusions may be made. First, most CSBs larger than 200m² are densely distributed in the new technological development zones. Totally, 2,257 CSBs are warehouses for factories and enterprises. Second, the CSBs smaller than 200m² are sparsely distributed in the urban villages, construction sites and the urban-rural junctions. Third, 4,002 temporary buildings are mainly built on residential buildings. As shown in Figure 9, number of small-sized buildings constitutes 61% (Fig. 9(a)) of all CSBs, while the area of large-size buildings constitutes 81% of the total floor area of all CSBs (Fig. 9(b)).

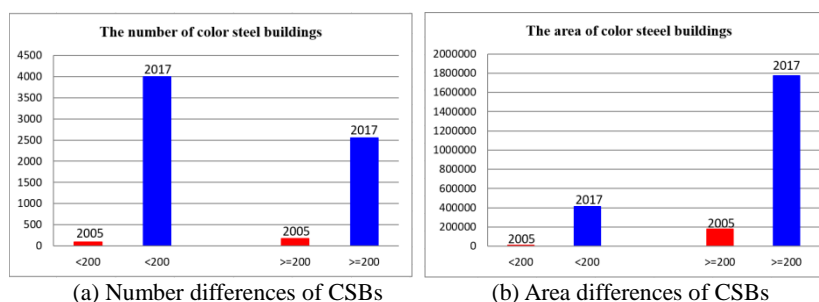
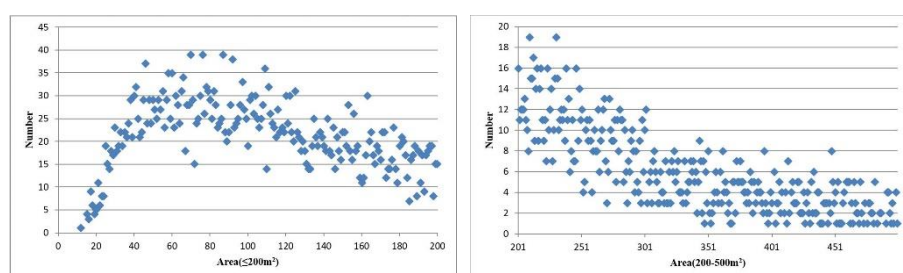


Fig. 9. Statistical analysis of the CSBs in 2005 and 2017

Since the number of CSBs in 2005 was too small, the data of 2017 was used for further analysis. According to field surveys, the area and the corresponding quantities of CSBs were provided in Fig. 10. Among the buildings in 2017, a large amount of CSBs is smaller than 200 m², and their spatial distribution is very concentrated. These buildings, mainly temporary buildings, carports, are built on the top of residential buildings in city villages. The CSBs with areas of 200-500 m² take 27% and are mainly scattered in the villages and their surroundings, including carports, small warehouses and small workshops. The number of CSBs larger than 500m² is relatively small, they are mainly located in the high-tech development zone and involve large warehouses and factories.



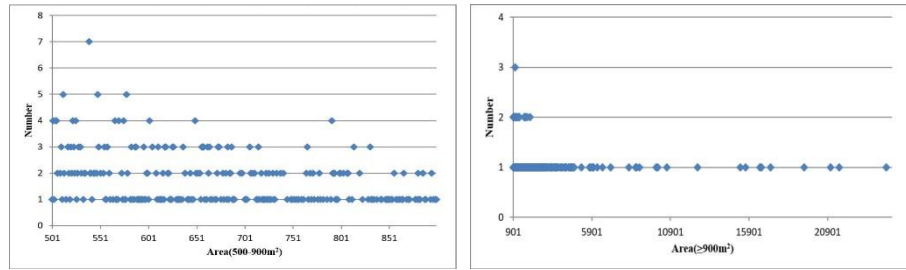


Fig. 10. Number of different types of CSBs in different areas in 2017

4.2 Spatial aggregation characteristics of CSBs

According to the previous study, only a small amount of CSBs was constructed in 2005, and the number of samples required for analyzing of spatial aggregation characteristics was not available. Therefore, we used 6,559 CSBs in 2017 as a sample in order to analyze the kernel density and spatial proximity characteristics.

4.2.1 KDE analysis

According to the extracted data, an empirical calculation method is adopted by the kernel density bandwidth (h) based on the aggregation characteristics and spatial distribution of CSBs [45].

$$h = 0.9 \times \min(S_D, \sqrt{\frac{1}{\ln 2} \times D_m}) \times n^{-0.2} \quad (3)$$

where n is the amount of CSBs, D_m is the median distance from the average center of each CSB to each CSB, and S_D is the standard distance.

First, the kernel density adopts the bandwidth of 200m to estimate the CSB data. The results are depicted in Figure 11. In the study area, the spatial distribution and aggregation characteristics of the CSBs are effectively displayed in the kernel density map. It can be observed from Figure 11 that the densely distributed areas of the CSBs were mainly found in two types of areas: the area surrounding universities, colleges and schools, and the area around some large factories, enterprises and companies. Because of the concentration of people and logistics in the schools and surrounding areas, fixed-construction buildings' rent is relatively high. Therefore, in the surrounding areas most of which are urban villages, the temporary CSBs are more concentrated in order to increase rent income because of high population density. Many factories and warehouses are located in factory-intensive and enterprise-intensive areas. These buildings are mostly large-area fixed CSBs.

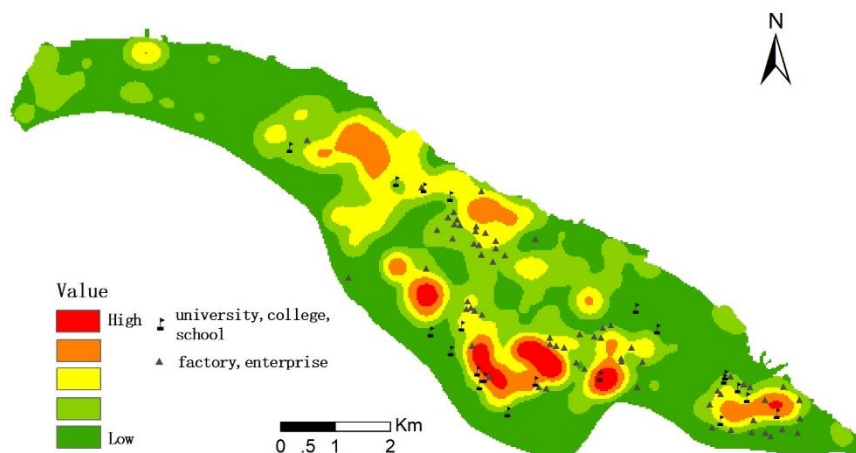


Fig. 11. Distribution of kernel density at the geometric center of CSBs

Second, the CSBs' areas were utilized by the kernel density as the weight according to above calculations, and the bandwidth was 200m. The results are depicted in Figure 12. We considered spatial distribution and aggregation characteristics of CSBs and spatial distribution characteristics of different types of CSBs. From the figure, large factories, enterprises and companies have the highest kernel density; among them, areas with the most obvious aggregation features are located in the streets of Mogao Avenue, Zhongbang Avenue, Lanke Road in the Anning New Technology Development Zone of Lanzhou City.

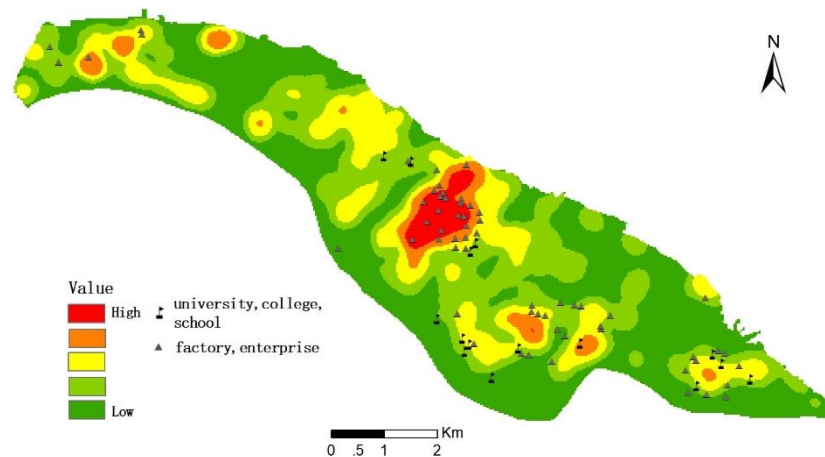


Fig. 12. Distribution of kernel density in the CSBs' area

4.2.2 Spatial proximity analysis

The previous sections of this paper show that CSBs have relatively high aggregation characteristics, especially obvious for the temporary small CSBs. For further study the aggregation and proximity characteristics of the temporary CSBs, a Delaunay-Voronoi method was used. In the experiment, we first calculated the geometric centers of all CSBs (Figure 13(a)). Second, based on the constrained Delaunay triangulation algorithm, we utilized the geometric centers of CSBs as the vertices (Figure 13(b)) to generate Delaunay triangulations. The spatial distribution and aggregation characteristics of the CSBs in Figure 13(a) can be effectively described by these Delaunay triangulations. Finally, Voronoi diagrams are generated based on a Delaunay triangulation (Figure 13(c)). The smaller areas of polygons in the Voronoi diagram indicate that the density of CSBs is higher, and the aggregation characteristics thereof are stronger.

In order to further quantify the proximity characteristics of CSBs, the Delaunay's side lengths (the distance between the geometric centers of CSBs) and the corresponding amounts in Figure 13(b) were analyzed (Figure 13(d)). The results show that the distance between the centers of the CSBs is generally about 20 meters, indicating that the CSBs have a very high adjacency characteristic.

Through the analysis of spatial proximity characteristics of the CSBs, combined with field surveys, we found that many of the CSBs located in urban villages around some schools (university, higher vocational school, high school, and elementary school) are very dense, which reflects the most obvious aggregation characteristics. Moreover, the boundary of the Voronoi diagram is identical to the boundary of a city village.

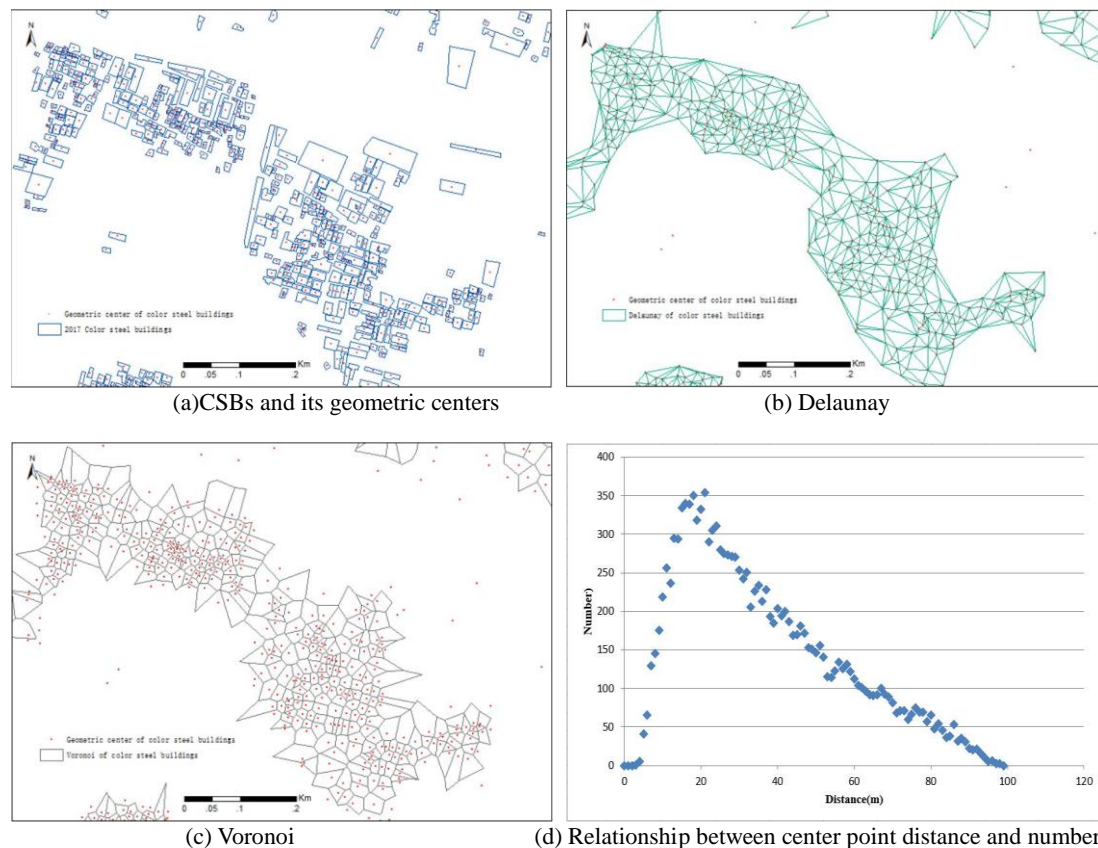


Fig. 13. Analysis of spatial proximity of CSBs

5. Conclusions

In a case study site of Western China, we extracted and analyzed CSBs according to remotely-sensed data. In this paper, the spatial distribution and aggregation characteristics of the CSBs can be analyzed by KDE, and the aggregation of various kinds of CSBs can be disclosed by using KDE through area classification. Based on the Delaunay-Voronoi method, we analyzed the spatial aggregation characteristics and the proximity of temporary CSBs. It was found that these buildings are mainly concentrated in shanty towns, urban fringes and urban villages. This shows that the transitional stage of urbanization is still undergoing. Therefore, some characteristics of the villages and towns still match those of the community.

In the study area, fixed CSBs with a large area are mainly located in the new technological development zone. Therefore, they are relatively concentrated, and a temporary CSB is smaller than the overall, indicating that the study area is undergoing the industrialization and the commercialization at a certain scale.

In the follow-up research, two areas of improvement are suggested below: (1) The streets with grid features divide the CSBs. Hence, network kernel density and other estimation methods can be utilized by the subsequent research work to more effectively analyze the aggregation characteristics and spatial distribution of CSBs. (2) As the risk of fire and public security often occur in temporary CSBs zone, we plan to research and analyze possible correlations between CSBs aggregation characteristics and fire. Typical study examples include population structure, population proportion, fire passages of areas where the temporary CSBs are densely distributed.

Acknowledgements: This research is supported by the National Key R&D Program of China (No.2017YFB0504201, and No.2017YFB0504203) and the National Natural Science Foundation of China (No. 41761082).

Author Contributions: Shuwen Yang designed the analytical framework, and wrote and revised the paper. Haowen Yan co-wrote and revised the paper. Yikun Li analyzed the data and polished the paper. Yi He. assisted the collection of research data. All authors read and approved the final

manuscript.

Conflicts of Interest: The authors declare no conflict of interest.

References

1. Woo, M.; Guldmann, J.M. Impacts of urban containment policies on the spatial structure of US metropolitan areas. *Urban Studies*. **2011**, *48(16)*, 3511-3536.
2. Zhong, C.; Arisona, S.M.; Huang, X.; Batty, M.; Schmitt, G. Detecting the dynamics of urban structure through spatial network analysis. *International Journal of Geographical Information Science*. **2014**, *28(11)*, 2178-2199.
3. Li, R. Study of Rail Transit and Urban Spatial Structure Based on Urban Economics. *Urban Transportation & Construction*. **2015**, *2*, 20-22.
4. Clifton, K.; Ewing, R.; Knaap, G.J.; Song, Y. Quantitative analysis of urban form: a multidisciplinary review. *Journal of Urbanism*. **2008**, *1(1)*, 17-45.
5. Gong, H.; Wheeler, J.O. The location and suburbanization of business and professional services in the Atlanta area. *Growth and Change*. **2002**, *33(3)*, 341-369.
6. She, B.; Zhu, X.; Ye, X.; Guo, W.; Su, K.; Lee, J. Weighted network Voronoi Diagrams for local spatial analysis. *Computers, Environment and Urban Systems*. **2015**, *52*, 70-80.
7. Talen E.; Wheeler S.M.; Anselin L. The social context of US built landscapes. *Landscape and Urban Planning*. **2018**, *177*: 266-280.
8. Batty, M. The size, scale, and shape of cities. *Science*. **2008**, *319(5864)*, 769-771.
9. Lan, Y.; Zhan, Q. How do urban buildings impact summer air temperature? The effects of building configurations in space and time. *Building and Environment*. **2017**, *125*: 88-98.
10. Yang, S.W.; Ma, J.J.; Wang, J.M. Reserch on Spatial and Temporal Distribution of Color Steel Building Based on Multi-Source High-Resolution Satellite Imagery. *ISPRS-International Archives of the Photogrammetry, Remote Sensing and Spatial Information Sciences*. **2018**, 2101-2105.
11. Hamada, S.; Ohta, T. Seasonal variations in the cooling effect of urban green areas on surrounding urban areas. *Urban forestry & urban greening*. **2010**, *9(1)*, 15-24.
12. Shi, K.; Yu, B.L.; Huang, Y.X.; Hu, Y.J.; Yin, B.; Chen, Z.Q.; Chen, L.J.; Wu, J.P. Evaluating the ability of NPP-VIIRS nighttime light data to estimate the gross domestic product and the electric power consumption of China at multiple scales: A comparison with DMSP-OLS data. *Remote Sensing*. **2014**, *6(2)*, 1705-1724.
13. Wei, Y.; Liu, H.; Song, W.; Yu, B.; Xiu, C. Normalization of time series DMSP-OLS nighttime light images for urban growth analysis with pseudo invariant features. *Landscape and Urban Planning*. **2014**, *128*, 1-13.
14. Herold, M.; Scepan, J.; Clarke, K.C. The use of remote sensing and landscape metrics to describe structures and changes in urban land uses. *Environment and Planning A*. **2002**, *34(8)*, 1443-1458.
15. Yin, C.; Liu, Y.; Wei, X.; Chen, W. Road Centrality and Urban Landscape Patterns in Wuhan City, China. *Journal of Urban Planning and Development*. **2018**, *144(2)*, 05018009.
16. Liu, Z.; He, C.; Zhang, Q.; Huang, Q.; Yang, Y. Extracting the dynamics of urban expansion in China using DMSP-OLS nighttime light data from 1992 to 2008. *Landscape and Urban Planning*. **2012**, *106(1)*, 62-72.
17. Pandey, B.; Joshi, P.K.; Seto, K.C. Monitoring urbanization dynamics in India using DMSP/OLS night time lights and SPOT-VGT data. *International Journal of Applied Earth Observation and Geoinformation*. **2013**, *23*, 49-61.
18. Shen, Y.; e Silva, J.A.; Martínez, L.M. Assessing High-Speed Rail's impacts on land cover change in large urban areas based on spatial mixed logit methods: a case study of Madrid Atocha railway station from 1990 to 2006. *Journal of Transport Geography*. **2014**, *41*, 184-196.
19. Yin, M.; Bertolini, L.; Duan, J. The effects of the high-speed railway on urban development: International experience and potential implications for China. *Progress in planning*. **2015**, *98*, 1-52.
20. Chen, X. A Spatial and Temporal Analysis of the Socioeconomic Factors Associated with Breast Cancer in Illinois Using Geographically Weighted Generalized Linear Regression. *Journal of Geovisualization and Spatial Analysis*. **2018**, *2(2)*, 5, 2-16.

21. Yu, W.; Ai, T.; Shao, S. The analysis and delimitation of Central Business District using network kernel density estimation. *Journal of Transport Geography*. **2015**, *45*, 32-47.
22. Spencer, J.; Angeles, G. Kernel density estimation as a technique for assessing availability of health services in Nicaragua. *Health Services and Outcomes Research Methodology*. **2007**, *7*(3-4), 145-157.
23. Ni, J.; Qian, T.; Xi, C.; Rui, Y.; Wang, J. Spatial distribution characteristics of healthcare facilities in Nanjing: Network point pattern analysis and correlation analysis. *International journal of environmental research and public health*. **2016**, *13*(8), 833.
24. Nakaya, T.; Yano, K. Visualising Crime Clusters in a Space-time Cube: An Exploratory Data-analysis Approach Using Space-time Kernel Density Estimation and Scan Statistics. *Transactions in GIS*. **2010**, *14*(3), 223-239.
25. Gerber, M.S. Predicting crime using Twitter and kernel density estimation. *Decision Support Systems*. **2014**, *61*, 115-125.
26. Ye, X.; Wu, L.; Lee, J. Accounting for Spatiotemporal Inhomogeneity of Urban Crime in China. *Papers in Applied Geography*. **2017**, *3*(2), 196-205.
27. Amenta, N.; Bern, M. Surface reconstruction by Voronoi filtering. *Discrete & Computational Geometry*. **1999**, *22*(4), 481-504.
28. Yan, H.; Li, J. An approach to simplifying point features on maps using the multiplicative weighted Voronoi diagram. *Journal of Spatial Science*. **2013**, *58*(2), 291-304.
29. Miao, Z.; Chen, Y.; Zeng, X.; Li, J. Integrating spatial and attribute characteristics of extended Voronoi diagrams in spatial patterning research: A case study of Wuhan City in China. *ISPRS International Journal of Geo-Information*. **2016**, *5*(7), 120.
30. Adrienko, N.; Adrienko, G. Spatial generalization and aggregation of massive movement data. *IEEE Transactions on visualization and computer graphics*. **2011**, *17*(2), 205-219.
31. Ryu, H.; Park, I. K.; Chun, B. S.; Chang, S. I. Spatial statistical analysis of the effects of urban form indicators on road-traffic noise exposure of a city in South Korea. *Applied Acoustics*. **2017**, *115*, 93-100.
32. Mo, W.; Wang, Y.; Zhang, Y.; Zhuang, D. Impacts of road network expansion on landscape ecological risk in a megacity, China: A case study of Beijing. *Science of the Total Environment*. **2017**, *574*, 1000-1011.
33. Shi, X.M.; Qin, M.Z. Research on the Optimization of Regional Green Infrastructure Network. *Sustainability*. **2018**, *10*, 4649.
34. Zhang, X.; Li, W.; Zhang, F.; Liu, R.; Du, Z. (2018). Identifying Urban Functional Zones Using Public Bicycle Rental Records and Point-of-Interest Data. *ISPRS International Journal of Geo-Information*. **2018**, *7*(12), 459.
35. Elgammal, A.; Duraiswami, R.; Harwood D.; Davis, L.S. Background and foreground modeling using nonparametric kernel density estimation for visual surveillance. *Proceedings of the IEEE*. **2002**, *90*(7), 1151-1163.
36. Xie, Z.; Yan, J. Kernel density estimation of traffic accidents in a network space. *Computers, environment and urban systems*. **2008**, *32*(5), 396-406.
37. Wenhao, Y. U.; Tinghua, A. I.; Pengcheng, L. I. U.; Yakun, H. E. Network Kernel Density Estimation for the Analysis of Facility POI Hotspots. *Acta Geodaetica et Cartographica Sinica*. **2015**, *44*(12), 1378-1383.
38. Wang, Z.; Ye, X.; Tsou, M. H. Spatial, temporal, and content analysis of Twitter for wildfire hazards. *Natural Hazards*. **2016**, *83*(1), 523-540.
39. Davies, T.M.; Hazelton, M.L. Adaptive kernel estimation of spatial relative risk. *Statistics in Medicine*. **2010**, *29*(23), 2423-2437.
40. Chen, P.Y.; Zhu, X.G. Regional inequalities in China at different scales. *Acta Geographica Sinica*. **2012**, *67*(8): 1085-1097.
41. Tobler, W. On the first law of geography: A reply. *Annals of the Association of American Geographers*. **2004**, *94*(2), 304-310.
42. Liebling, T.M.; Pournin, L. Voronoi diagrams and Delaunay triangulations: Ubiquitous siamese twins. *Documenta Mathematica, ISMP*. **2012**, 419-431.
43. Lam, M.C. Maximizing survey volume for large-area multi-epoch surveys with Voronoi tessellation. *Monthly Notices of the Royal Astronomical Society*. **2017**, *469*(1), 1026-1035.
44. Ebeida, M.S.; Mitchell, S.A.; Davidson, A.A.; Patney, A.; Knupp, P. M.; Owens, J. D. Efficient and good Delaunay meshes from random points. *Computer-Aided Design*. **2011**,

- 43(11), 1506-1515.
45. Davies, T.M.; Flynn, C.R.; Hazelton, M.L. On the utility of asymptotic bandwidth selectors for spatially adaptive kernel density estimation. *Statistics & Probability Letters*. **2018**, *138*, 75-81.